Chapter 5

RACM of Inverters: Walsh Function based KNN Approach

5.1 Introduction

The previous chapter has discussed the PCA-WE-SVM technique, which can detect the OC faults in a single IGBT and multiple IGBTs of inverters. For feature extraction, the WE technique is more accurate and simpler with a less computational burden. The SVM algorithm gives accurate fault diagnosis results using the WE feature of three-phase currents of the inverter. The fault detection and localization time with the proposed technique are found in lesser execution time than the other techniques available in the literature. The detection time of the open-circuit fault of IGBTs-based inverter can be further decreased, and accuracy can be improved with other supervised based machine learning techniques or by combining the SVM technique with other feature extraction techniques. Therefore, this chapter is focused on the OC fault diagnosis system with WF based feature which helps in getting fastest and accurate diagnosis results. The block diagram representation of the RACM of inverter using the proposed OC fault diagnosis method is shown in Fig. 5.1. The KNN and MLP techniques are used for OC fault localization in this chapter.

There are various machine learning and signal processing techniques available in the literature for the improvement of power quality, voltage and current quality. The machine learning techniques are also seen in the fault diagnosis algorithms of various components of power system including transmission line, generators and transformers. Various frequency-domain techniques, such as the FFT and WT [52], as well as machine learning-based techniques, such

as RF, KNN, DA, NB, DT, PCA, and SVM [80–83], have been addressed in the literature. The defects in the converter module were diagnosed using these techniques. In [52], the WT technique was used to locate faults using converter three-phase currents. The FFT is often used in a frequency-domain dependent fault detection technique, but it does not do well in transient conditions.

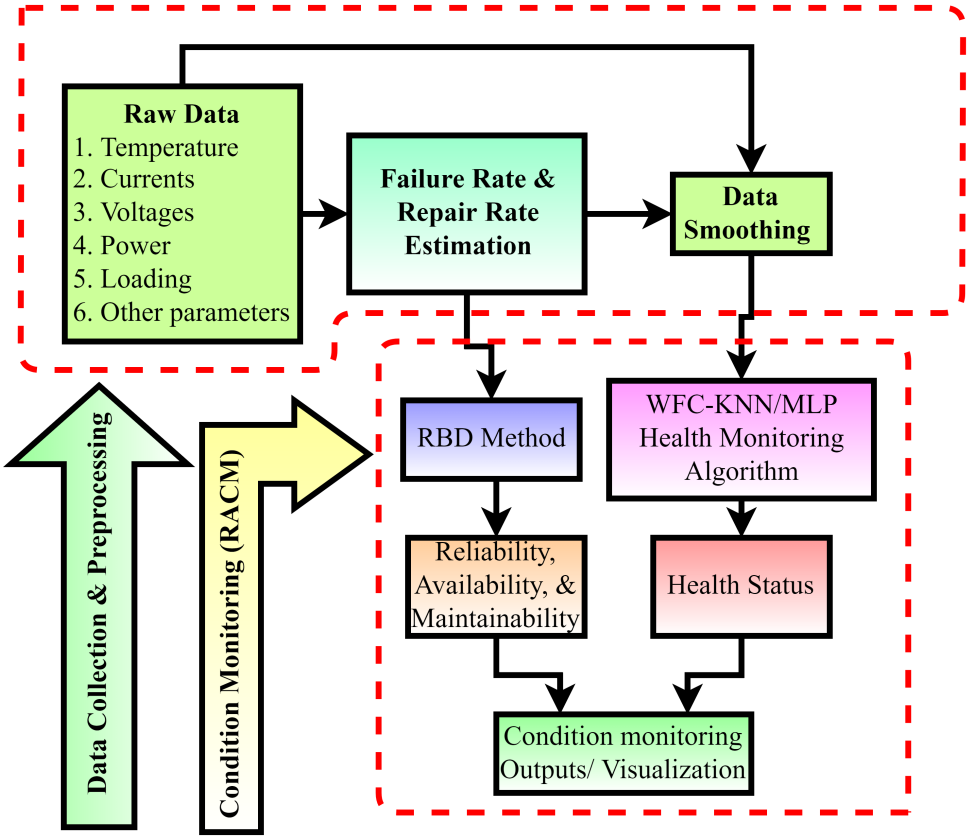

Figure 5.1: RACM using PCA-EWP-KNN technique.

MKSTM explained in [54], which uses the data of AC and internal circulation current for extracting the characteristics. The authors have discussed the neural network-based MLP technique, SVM, SOM, and K-means machine learning techniques in [52] for the fault classification and detection. The authors found the SVM technique as a better and accurate technique for fault classification. The voltage and current characteristics of IGBTs have been used to detect faults [59,61,65,99]. A fault detection system based on the ESO has been briefly explored [58]. This work identifies the defective sub-module, but it is unable to reveal the faulty switch. As a result, fault localization is also needed. The authors [84] suggested a fault diagnostic method based on the arm voltage and arm voltage error characteristics of the modular MLI sub-module. Within a few control cycles, the algorithm identifies and locates the fault. The OC faults detec-

tion algorithm is proposed in [85] using current and voltage characteristics. The authors have used characteristics such as an increase in phase current magnitude and a DC voltage reduction. Various control schemes, such as clustering of various potential faults and locations, are used to boost MLI's fault-tolerant capability [86]. Faults should be found as quickly as possible in order to enforce this form of fault-tolerant MLI.

In the literature, the prediction of OC faults in IGBTs using existing characteristics and a machine learning technique has been proposed. The authors [87] implemented the HHT for OC fault detection, followed by an ANN technique for fault localization. According to the literature, SVM outperforms ANN in terms of results. The PCA technique has been explored in some available literature [80–83]. Only the extraction and collection of data attributes are used in this methodology.

The selected features are then used in [80] to classify faults using classifier techniques. The study found that by using PCA as a feature extraction and selection technique, SVM takes longer to execute than other techniques such as RF, KNN, DA, NB, and DT. In terms of accuracy, however, the SVM approach has better performance during learning and testing time periods. The SVM technique's accuracy range is found to be 94.88% to 99.18%. According to the authors [83], the PCA-SVM technique is more accurate than other techniques such as PCA-ELM and PCA-DT.

The WFs are used to reduce the computational burden in the fault detection algorithm. These functions use only simple mathematical operations such as shifting and addition. These do not involve the complex mathematical operations such as multiplication, division, square, and square-root. The WF occupy the values +1 and -1 only which makes it more simpler than other complex algorithm which are based on Fourier series and Fourier transform [100, 101]. Therefore, it is possible to avoid the amount of real-time computational complexity by implementing a fast fault detection algorithm utilizing WFC for current or voltage waveform. Hence, WFC is a good and accurate feature for fault diagnosis algorithm. In the present work, the accuracy of fault diagnosis technique using proposed WFC-KNN algorithm is in the range of 99% to 100% which is better than that of WFC-SVM having accuracy in the range of 82% to 83.12%.

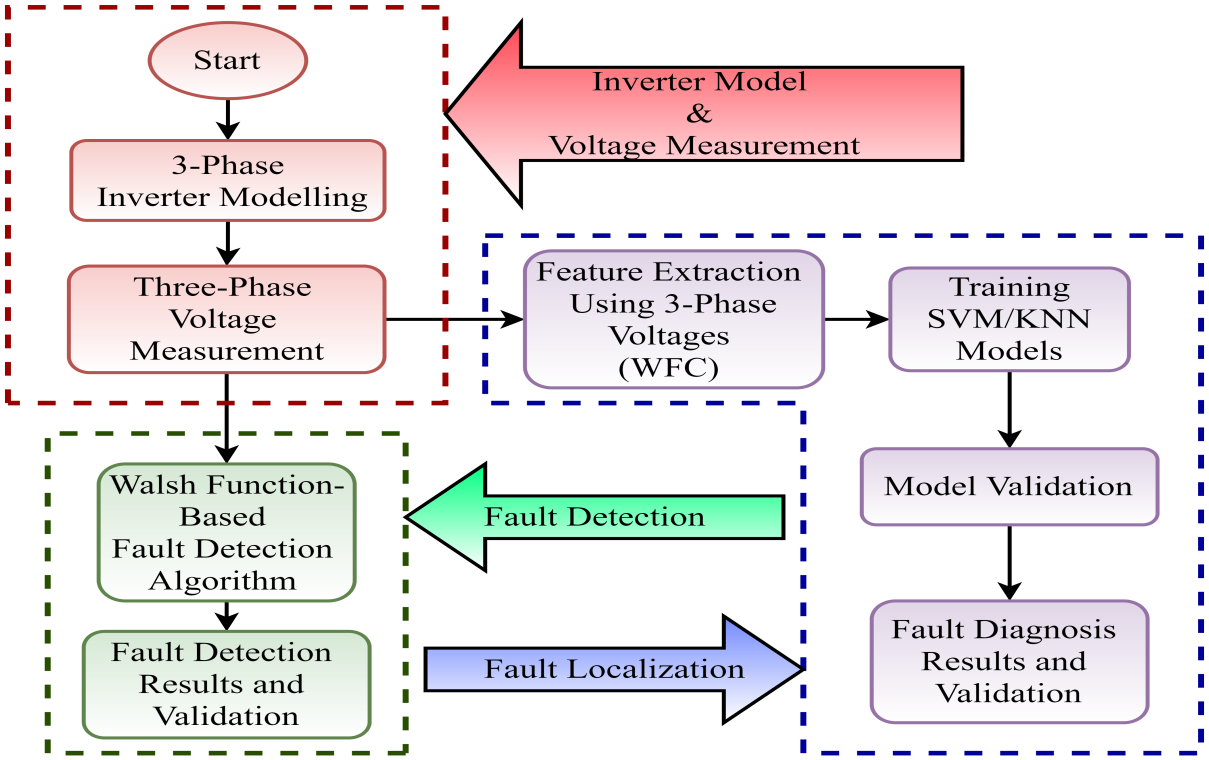

Figure 5.2: Process flow of the proposed algorithm

5.2 WFC-KNN Approach for RACM

Fig. 5.2 depicts the proposed algorithm's phase flow. This work simulates a three-phase inverter and uses the SPWM technique to produce triggering pulses. At the inverter's output, the three-phase voltages are measured. The WFC-based algorithm is used to detect OC faults in IGBTs using line voltages of three-phase inverter. The WFC is often used to classify faults and pinpoint where a OC switch is located. The SVM and KNN algorithm are then trained using the extracted features from the voltage signals. The learned SVM and KNN models are then tested for identification and classification of faults. The state of the inverter and its switches is indicated by the output of the SVM and KNN models.

Open-circuit faults are the most common faults in IGBTs and IGBT-based converters and inverters. A single open-circuit fault in a single IGBT will cause the entire inverter to fail. The protection of the inverters in a MMI is dependent on the fault detection and monitoring system of the IGBTs. As a result, IGBT fault detection and localization are important.

The collection and extraction of features is a vital part of machine learning-based fault diagnosis algorithms. Entropy, WT, mean, phase angle, and dq0 transition of the time series current or voltage waveform are among the most frequently proposed features in the litera-

ture [26–29]. Due to almost identical values with features of different fault conditions, these features do not have effective fault identification and may result in incorrect labelling of faults. The PCA technique has been referred to as a multivariate features extraction and selection technique by the majority of researchers in the literature [80–83]. PCA, on the other hand, is an unsupervised machine learning technique. Where the fault conditions are uncertain and no empirical evidence of fault cases is available, this approach is preferred. The PCA features which shift unpredictably as a result of the dynamic nature of load, and the classifier may become confused if it uses the features derived from the PCA technique. Any potential adjustment in loads, electrical device parameters, and inverters must be trained into the fault classification algorithm. In addition, extracting and selecting features for classification is a time-consuming process. As a result, the PCA-SVM or PCA-KNN technique has a longer execution time. The execution time of KNN and SVM techniques can be shortened by using other realistic feature extraction techniques. As a result, in this chapter, the WFC-based functionality is proposed, which is derived from the WF of current signals. Using the WFC as feature decreases computational and execution time, resulting in a quicker fault diagnosis response. In this chapter, the WFC-based algorithm is used to detect OC faults. It is observed from the results of KNN and SVM classification algorithms that KNN-based technique has better accuracy and faster response than SVM-based classification technique. Implementing the proposed fault detection technique (WFC) and classification technique (KNN) improves accuracy and reduces execution time.

5.2.1 Walsh-Function Coefficients (WFC)

The voltage or current waveform can be expanded by using WF. The WFCs ($W_p, p = 1, 2, ...$) are determined from the WF. In terms of WF, the current signal $i(t)$ can be written as given in eq. (5.1).

$$i(t) = \sum_{p=0}^{\infty} W_p Wal(p, \frac{t}{T}) \tag{5.1}$$

where, W_p is the p_{th} WFC whose value is determined by the eq. (5.2).

$$W_p = \frac{1}{T} \int_0^T i(t) Wal(p, \frac{t}{T}) dt \tag{5.2}$$

where, k=0,1,2, ...

Considering that there are N number of samples in one cycle of $i(t)$ and the sampling interval

Δt is related to the time period as $T = N\Delta t$. This way, the time at instant q is given by $t_q = q\Delta t$ where, q=0,1,2, ..., N and corresponding value of $i(t)$ is given by $i(t_q) = i(q\Delta t)$. Also, the value of Walsh function is determined from the eq. (5.3).

$$Wal(p, t_q^{'}) = Wal(p, \frac{q\Delta t}{T}) = Wal(p, q\Delta t^{'}) \tag{5.3}$$

where, $\Delta t^{'} = \frac{\Delta t}{T}$

Therefore, the WFC (W_p) is expressed as given in eq. (5.4).

$$W_p = \frac{1}{T}\int_0^T i(t).Wal(p, t^{'})dt \tag{5.4}$$

Using Trapezoidal rule for solving the eq. (5.4) and the relation of N and T, the p_{th} WFC is given as shown in eq. (5.5).

$$W_p = \frac{1}{N}[0.5g_0 + g_1 + ... + g_q + .. + g_{N-1} + 0.5g_N] \tag{5.5}$$

where, $g_q = i(t_q).Wal(p, q\Delta t^{'})$

The p_{th} WFC for each (k=1,2, . .) are evaluated for each coming sample of $i(t)$. Therefore, it is clear that the WFC is determined at each nearest instants and for calculating it only addition and shifting operations are used. This results in fast feature collection and reduced computational burden. Hence, this feature is able to detect the fault in very short time interval and give accurate results of fault localization when used as feature in classification techniques like SVM and KNN.

5.2.2 OC Fault Detection using WFC

Fig. 5.3 shows the line voltage V_{ab} of three-phase inverter under normal condition. Fig. 5.4 shows the line voltage V_{ab} under fault condition at IGBT S_1 occurring at time t=0.08 s. In fig. 5.5, the WFCs are shown for the normal voltage signal. The signal can be reconstructed accurately using the WFCs as shown in Figure 5.6. Hence, this shows that the WFCs are very effective feature of the voltage signals. This can be very useful to detect the fault condition.

The WFCs for voltage signal under S_1 fault is shown in fig. 5.7 where the WFCs are different as compared to that of normal condition. The new sample is collected and the old sample is shifted out from the window. This way, the WFCs also changes. The second, third and forth samples coming in one by one in the window and the corresponding WFCs are shown in figs. 5.8,5.9, and 5.10. Similarly, under S_1 fault condition, the WFCs of voltage signal for

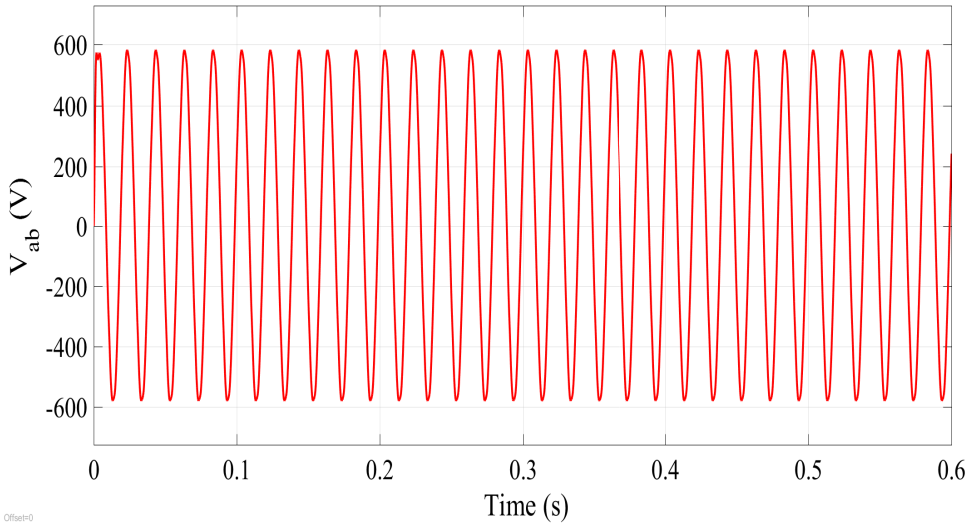

Figure 5.3: Line voltage V_{ab} under normal condition

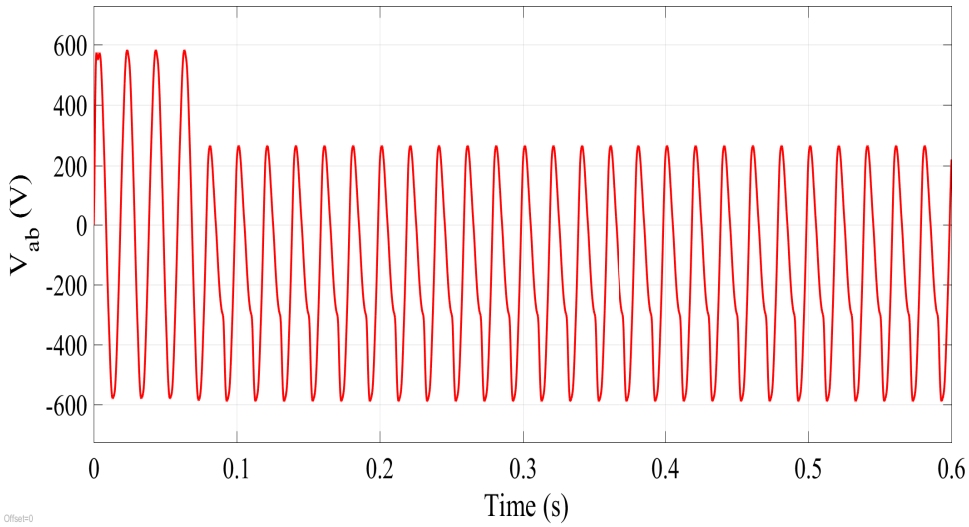

Figure 5.4: Line voltage V_{ab} under fault condition at S_1

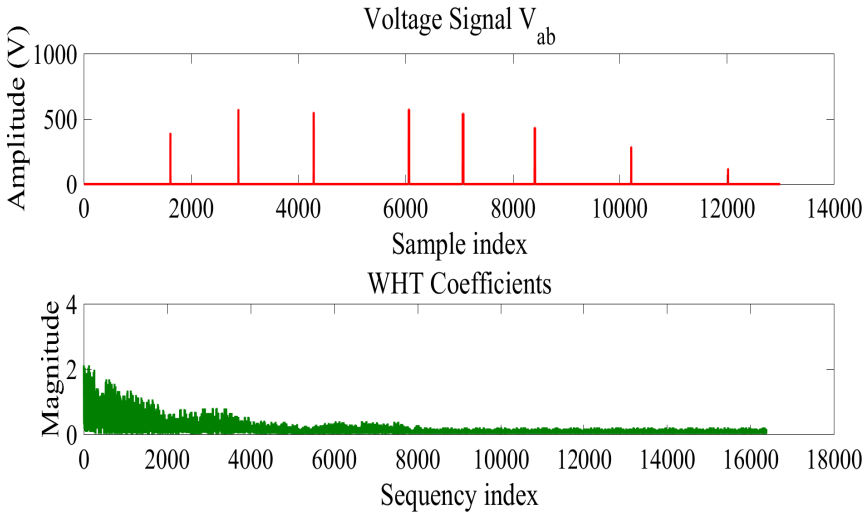

Figure 5.5: WFCs of voltage signal under normal condition

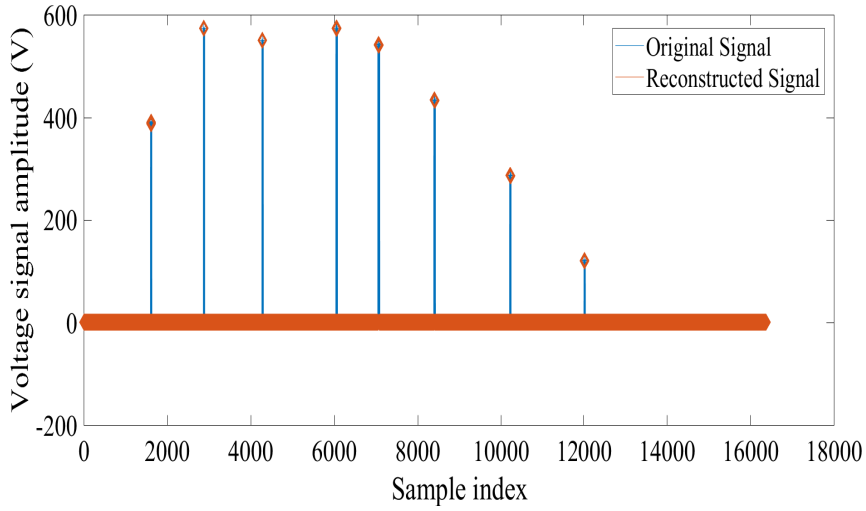

Figure 5.6: Reconstruction of voltage signal using WFCs

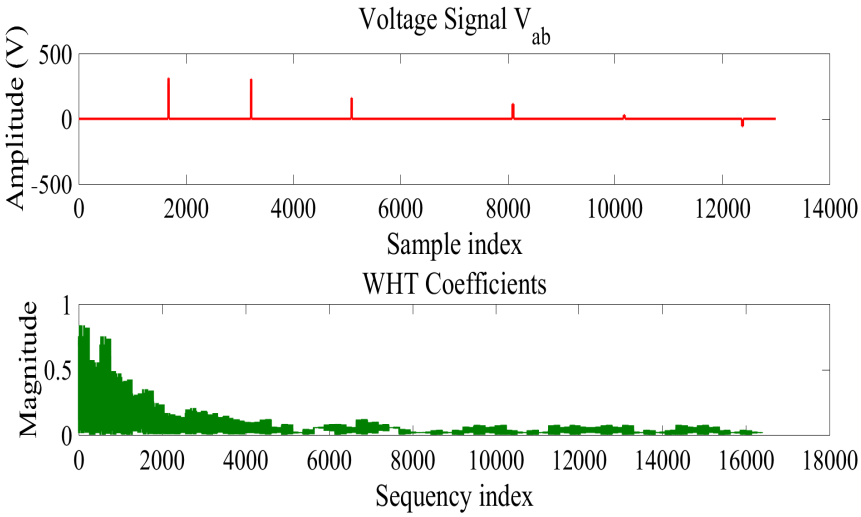

Figure 5.7: WFCs of voltage signal under fault condition in S_1

second, third and forth samples coming in are shown in figs. 5.11,5.12, and 5.13. When fig. 5.8 is compared with fig. 5.11, fig. 5.9 with fig. 5.12, and fig. 5.10 with fig. 5.13, the WFCs are found of different nature. This makes sense that WFCs are strong characteristics of the voltage signal to detect the fault and to be used as feature for fault classification.

The signal and its samples are changing in the window as new sample is added and old sample is shifted out. Therefore, WFCs will definitely vary even in normal condition for each new sample coming in. This is an important observation that simply WFCs can not be used to detect the fault. Therefore, an algorithm is developed in this research work to detect the fault in IGBTs of converters using the WFCs of the voltage signal. For this, an direct method of calculating magnitude and phase of WFCs is proposed. Using the particular selected WFCs, the magnitude and phase angle are calculated with each new sample coming in and old sample shifted out. The window is selected of 11 samples in the proposed algorithm. The first component (C_1) of magnitude is calculated using eq. 5.6 and second component (C_2) is calculated using eq. 5.7. The terms W_i stand for i_{th} WFC of voltage samples present in the window.

$$C_1 = 0.9W_1 - 0.373W_5 - 0.074W_9 \tag{5.6}$$

$$C_2 = 0.9W_2 + 0.373W_6 - 0.074W_{10} \tag{5.7}$$

For each new sample coming in the window of 11 samples, the magnitude (M) and phase (P) are calculated using the formula given in eqs. 5.8 and 5.9 respectively. These values are

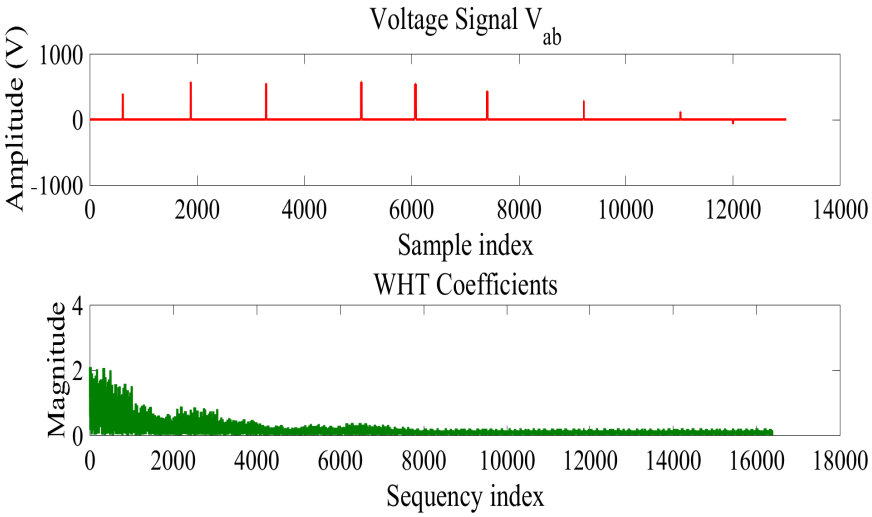

Figure 5.8: WFCs of voltage signal under normal condition with second next sample coming in.

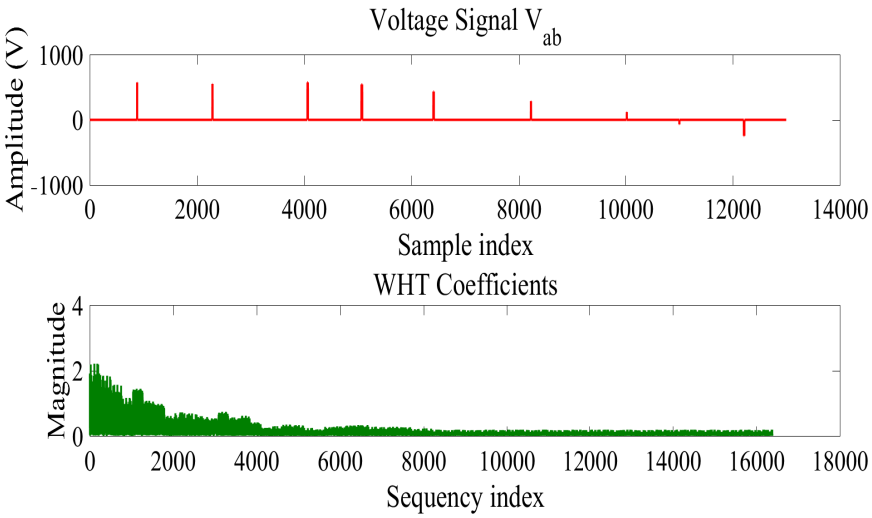

Figure 5.9: WFCs of voltage signal under normal condition with third next sample coming in.

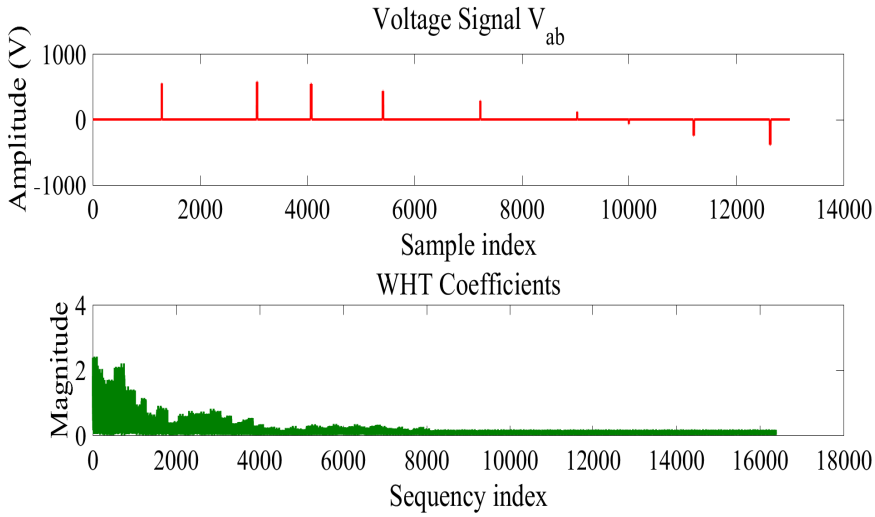

Figure 5.10: WFCs of voltage signal under normal condition with forth next sample coming in.

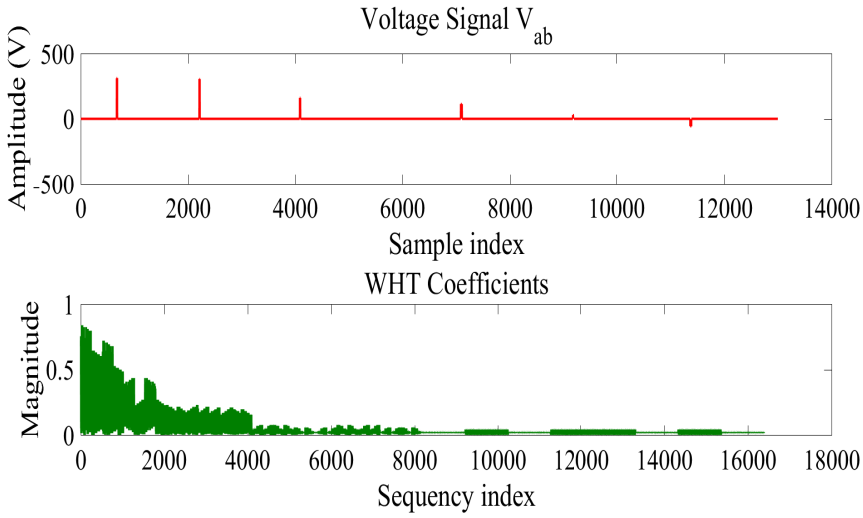

Figure 5.11: WFCs of voltage signal under S_1 fault condition with second next sample coming in.

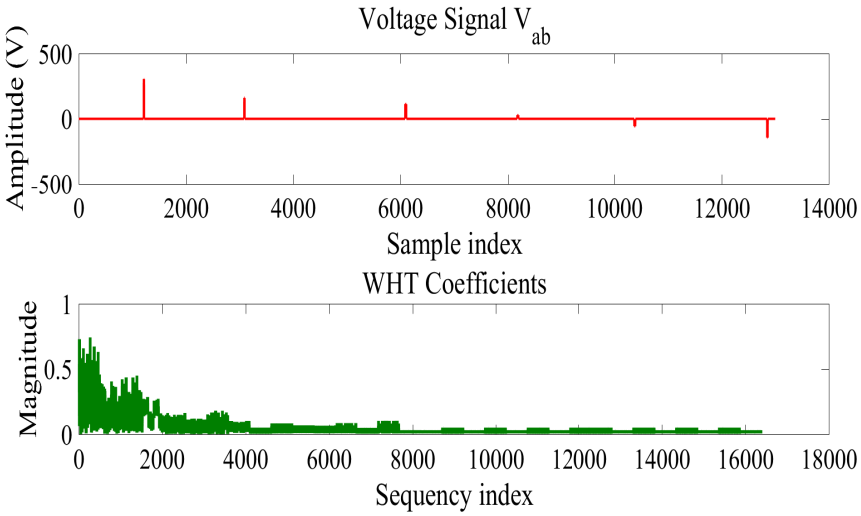

Figure 5.12: WFCs of voltage signal under S_1 fault condition with third next sample coming in.

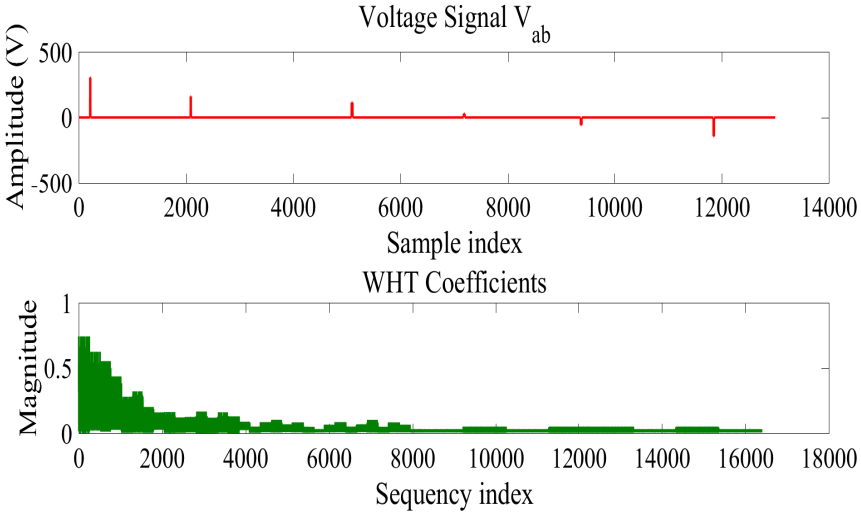

Figure 5.13: WFCs of voltage signal under S_1 fault condition with forth next sample coming in.

Figure 5.14: Magnitude of WFCs of window of 11 samples of voltage signal under normal condition.

approximately equal to the amplitude and phase angle of the fundamental component of the current signal.

$$M = \sqrt{2}\sqrt{C_1^2 + C_2^2} \tag{5.8}$$

$$P = tan^{-1}(C_2/C_1) \tag{5.9}$$

The magnitude and phase of WFCs of window of 11 samples under normal condition and fault condition at S_1 are shown in figs. 5.14 and 5.15. The magnitude and phase of WFCs of the window with different 11 samples after occurrence of fault at S_1 are shown in figs. 5.16 and 5.17. These figures show that the magnitude and phase of selected WFCs differ with the change in condition of the converter's switches.

The detection of fault under S_1 fault condition and generation of alarm are shown in fig. 5.18 and the zoomed view of the fault occurrence and detection are shown in fig. 5.19.

5.2.3 WFC-SVM and WFC-KNN Techniques for Fault Diagnosis

The WFC-SVM and WFC-KNN techniques are implemented for fault localization in parallel the fault is detected from the WFC-based detection algorithm. For this, WFC is used as a feature for the fault classification and localization.

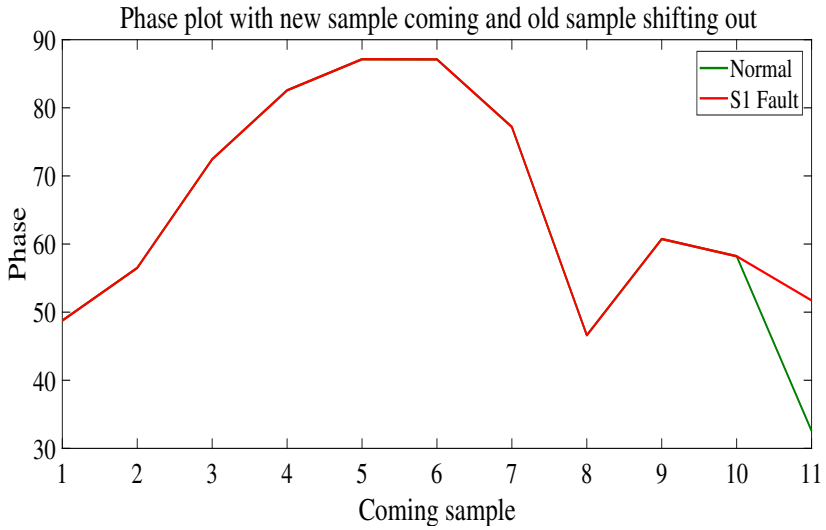

Figure 5.15: Phase of WFCs of window of 11 samples of voltage signal under normal condition.

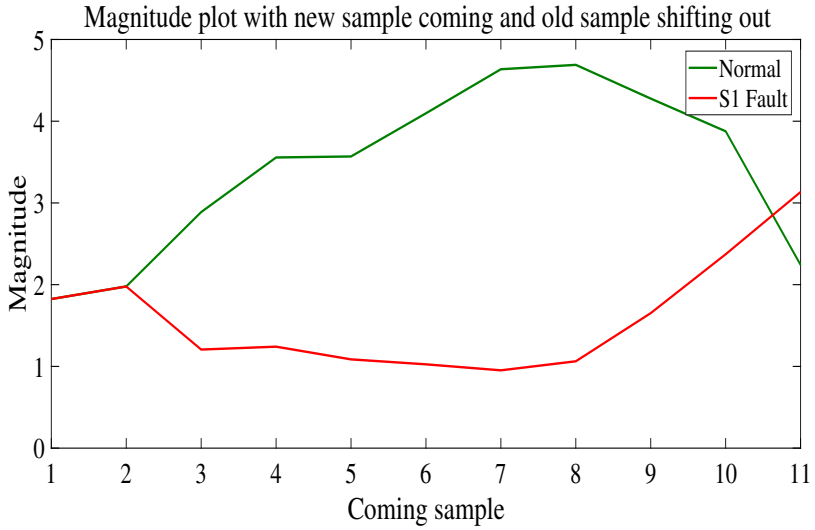

Figure 5.16: Magnitude of WFCs of window of 11 samples of voltage signal under fault condition at S_1.

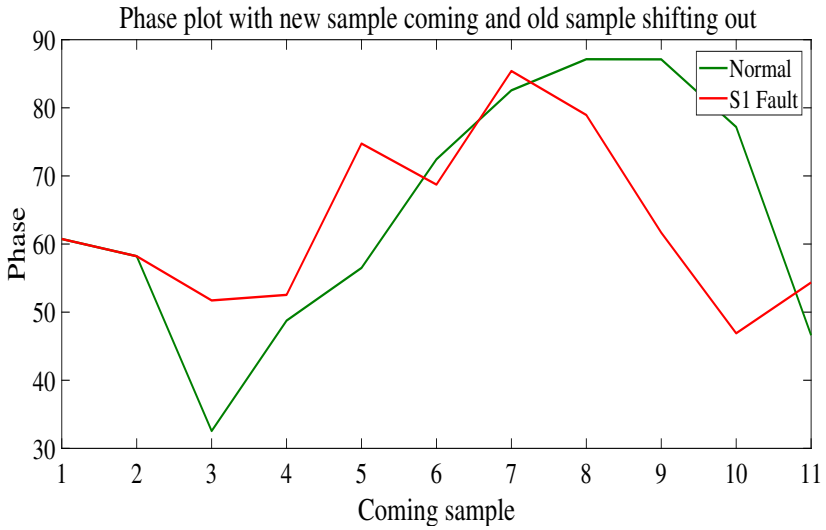

Figure 5.17: Phase of WFCs of window of 11 samples of voltage signal under fault condition at S_1.

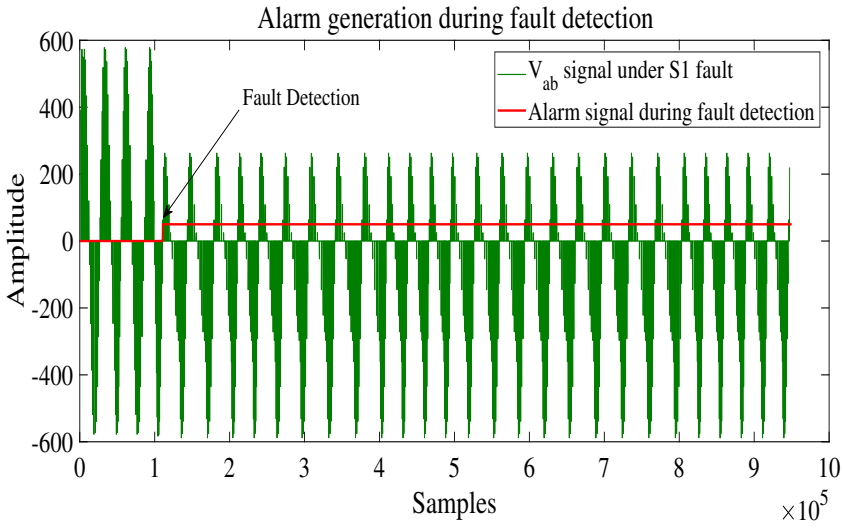

Figure 5.18: Fault detection and generation of alarm under fault condition at S_1.

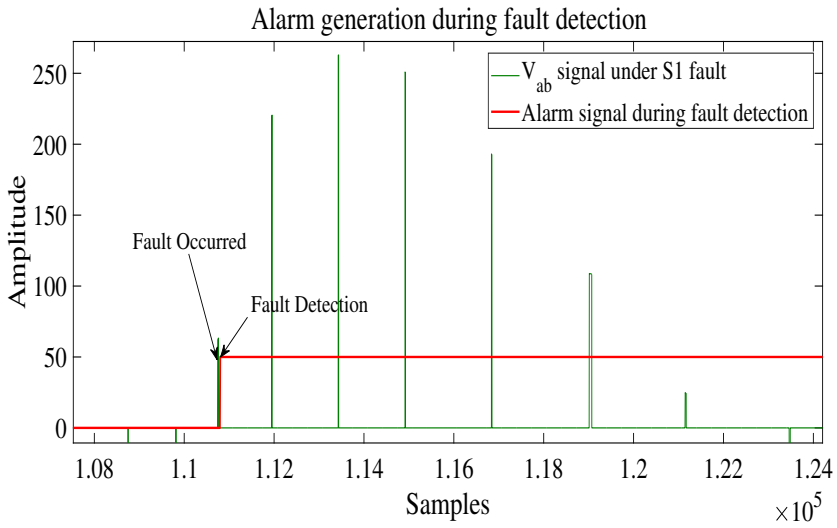

Figure 5.19: Zoomed view of occurrence of fault, detection and generation of alarm under fault condition at S_1.

The fault classification result using magnitude and phase as features of SVM-based algorithm, fine KNN and Weighted KNN are shown in figs. 5.20, 5.21, and 5.22. These results are obtained when the models are trained with normal data and faulty data under OC fault in single IGBT.

5.3 Results and Discussion

The simulation model is run under different possible loading conditions and faults, including single IGBT OC fault and multiple IGBTs OC faults. The voltage measurement data is used to detect the OC faults using WF and extract the WFC feature to train the SVM and KNN model for fault diagnosis. After training the SVM algorithm, it is validated for different faults in the inverter, and it is found that the WFC-SVM model gives accurate fault detection results with accuracy in the range of 81.58% to 83.12% as shown in fig. 5.23. The accuracy of KNN-based classification technique is found to be more than SVM in the range of 99.08% to 100% as shown in fig. 5.24.

The accuracy of MLP-based classification technique is found to be more than KNN in the range of 99.13% to 100% as shown in fig. 5.25.

Once the fault is detected, the KNN or MLP-based fault localization techniques, which are superior, outputs the faulty IGBT location, which also takes very less time because of the less computational burden involved in the WFC feature. This results in a fastest fault diagnosis

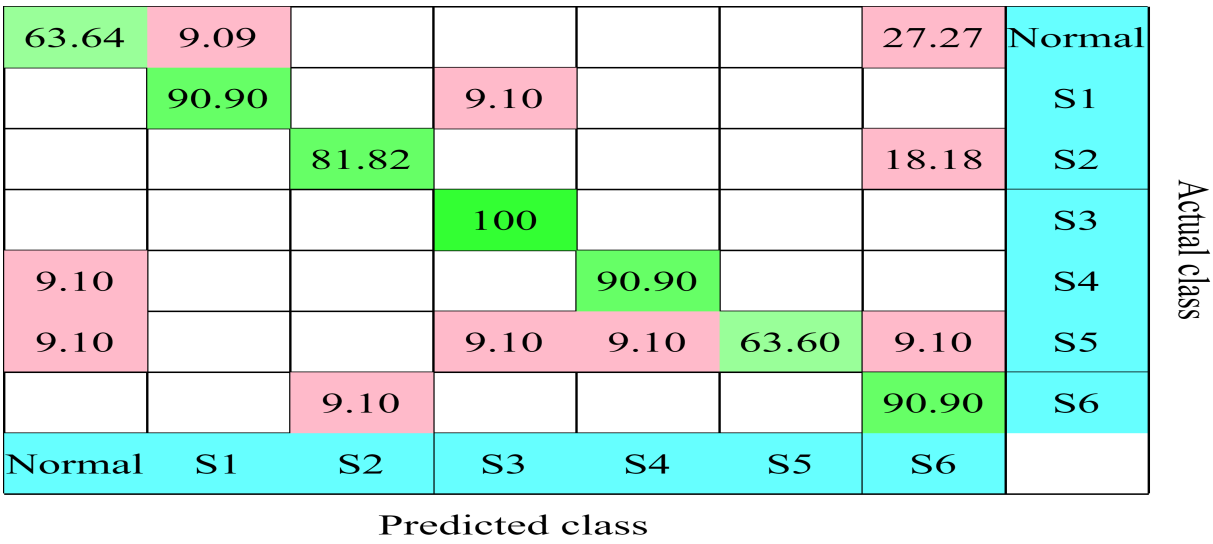

Figure 5.20: Fault classification result using SVM-algorithm

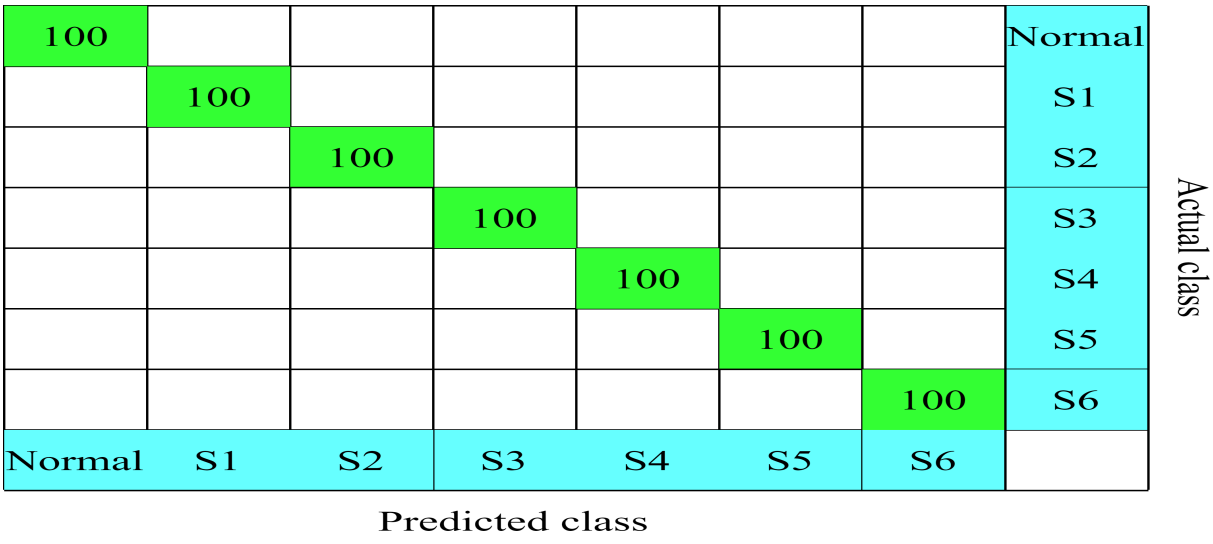

Figure 5.21: Fault classification result using fine KNN-algorithm

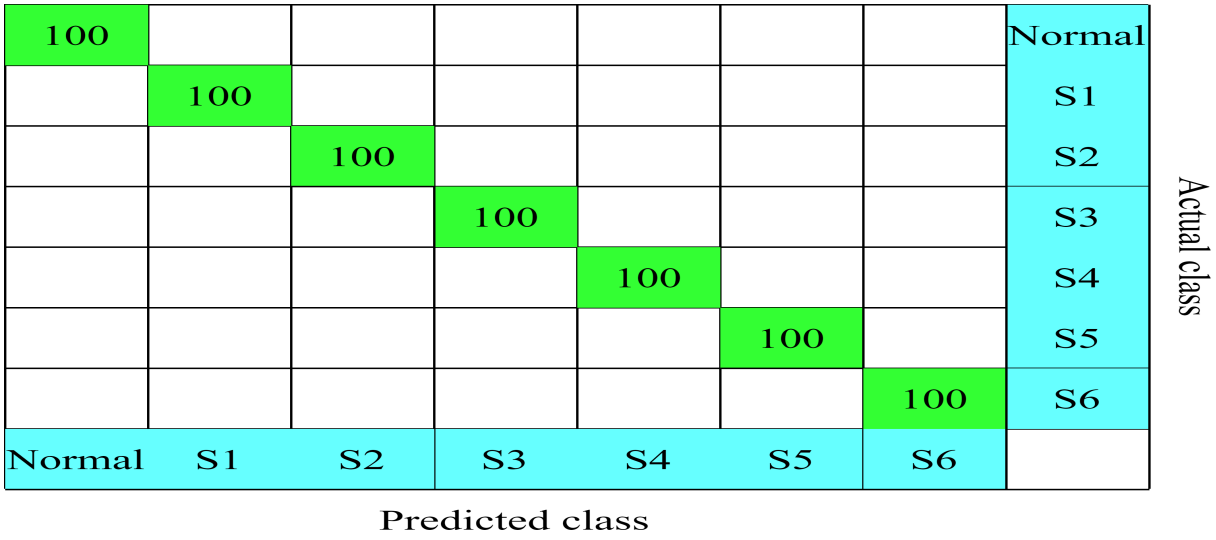

Figure 5.22: Fault classification result using weighted KNN-algorithm

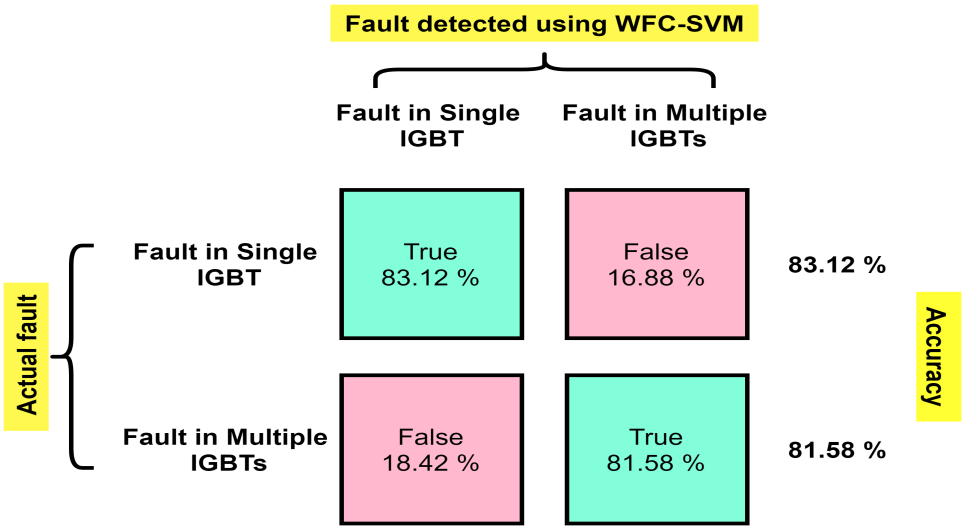

Figure 5.23: Accuracy of SVM-based fault classification technique

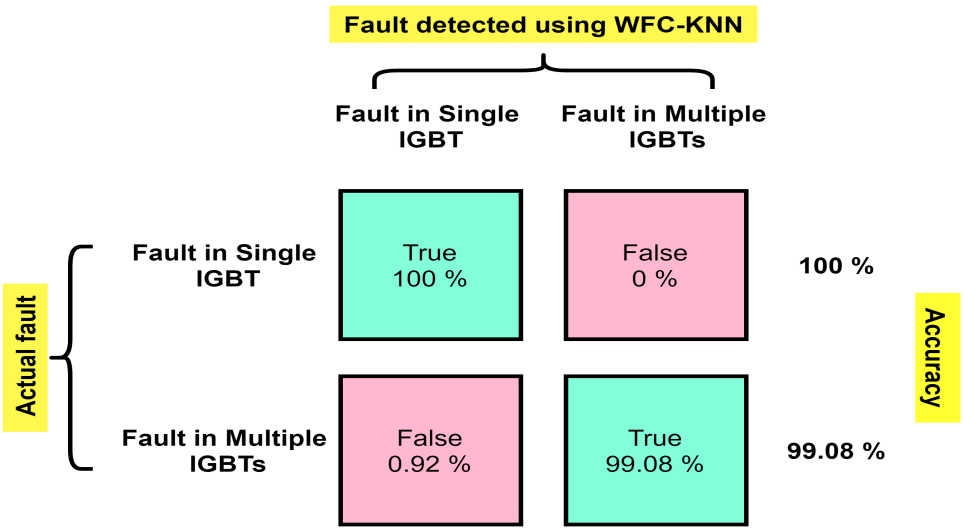

Figure 5.24: Accuracy of KNN-based fault classification technique

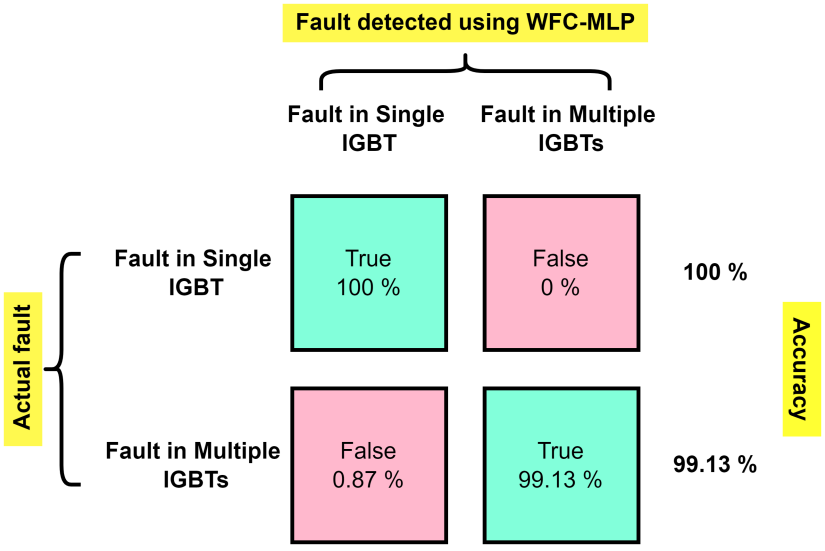

Figure 5.25: Accuracy of MLP-based fault classification technique

Table 5.1: Training time for KNN and SVM classification techniques

Classification technique	Computational time (micro-s)	Accuracy (%)
SVM	0.43532	82.58-83.12
Fine KNN	0.94921	98-100
Weighted KNN	0.1419	99.08-100

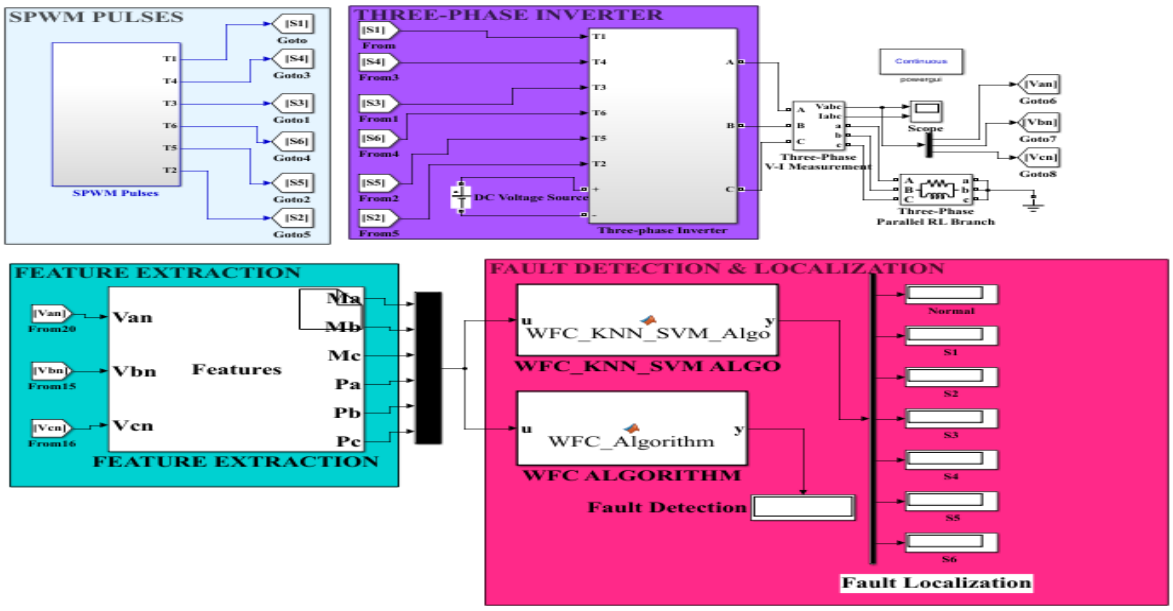

Figure 5.26: Prototype for the proposed algorithm of fault detection and localization.

system.

The training time and accuracy of SVM and KNN-based fault classification techniques are measured from MATLAB software and tabulated in Table 5.1. It is observed that the weighted KNN technique has lowest training time and gives 100% accuracy.

The Simulink model of the proposed work is shown in Fig. 5.26 as prototype. The voltage of each phase is measured for feature extraction and fault detection. The detection part is done by the walsh function-based detection algorithm and the localization of the faulty switches is done by WFC-SVM based algorithm. This chapter is focused on fault detection and localization only. The disabling of triggering pulses of IGBTs is not done in this chapter as redundant inverter switches are not used. Under normal working condition of the inverter, the fault detection and localization results are shown in Fig. 5.27. Whenever there would be fault in switches, the particular output block will indicate the same as shown in Fig. 5.28.

By using eqs 2.19 and 2.20 of chapter two, and Table 2.3, the reliability of the sub-systems

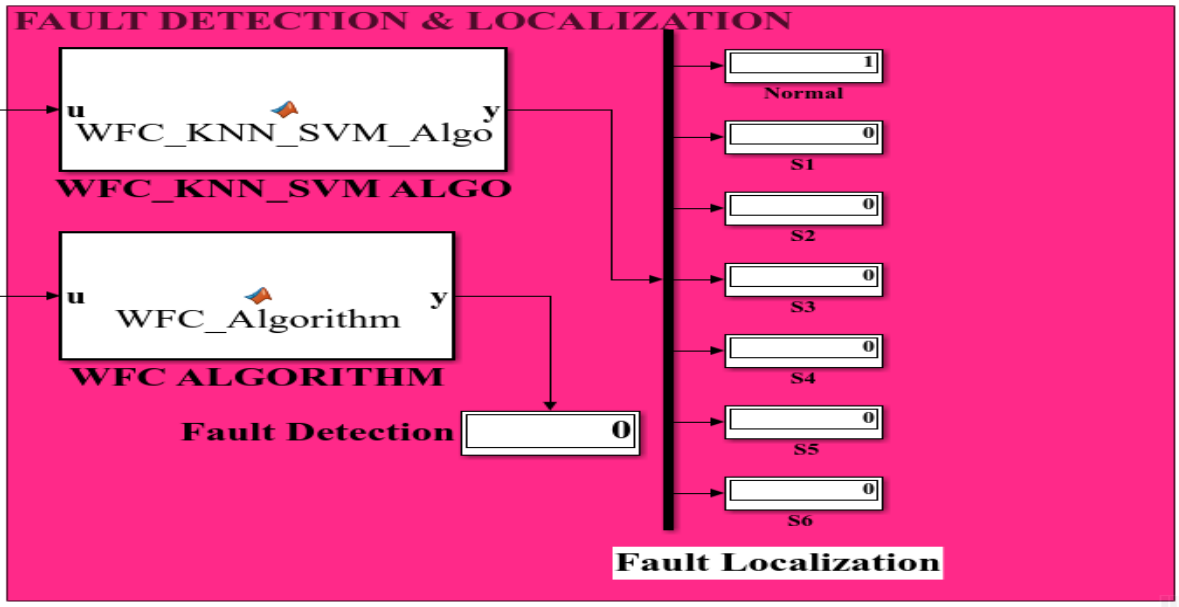

Figure 5.27: Outputs of fault detection and localization algorithms under normal condition.

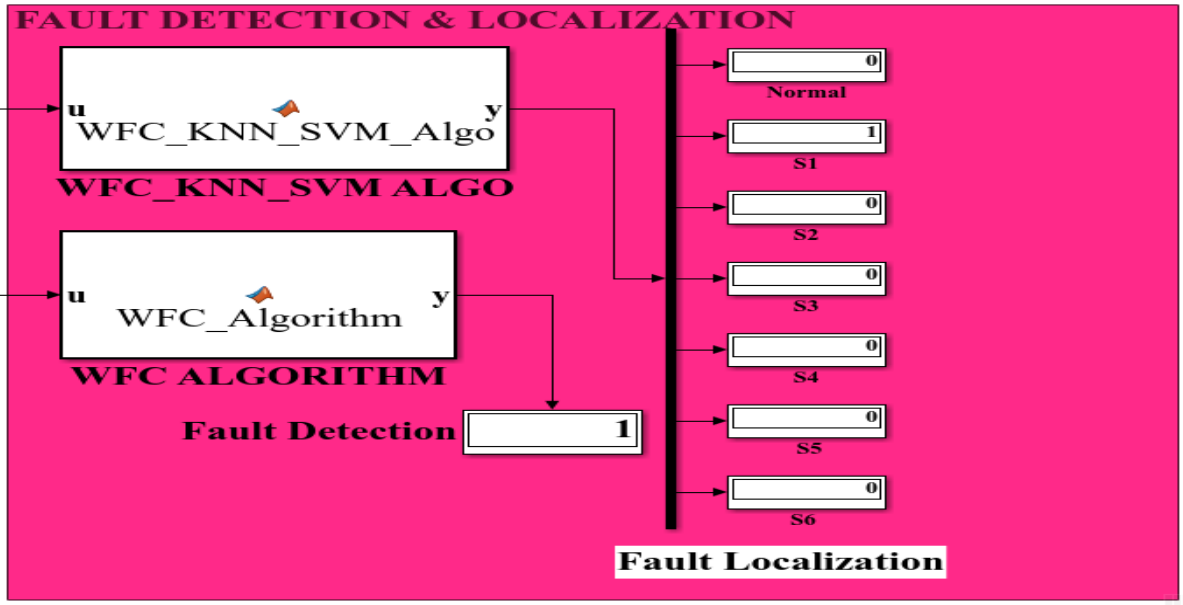

Figure 5.28: Outputs of fault detection and localization algorithms under fault condition in switch S1.

Table 5.2: Subsystem reliability of PV system for one year of operation (in %) (using eq 2.19)

Power (in kW)	100	200	500	1000	1500	2000	2500
PV modules	97.9869	96.0142	90.4114	81.6699	73.8389	66.6997	60.3041
converter	93.6925	87.7828	72.1977	55.6342	40.1666	28.9993	20.9368
Inverter	88.3292	78.0204	53.7676	32.7293	17.5977	9.4619	5.0874
BOS	92.5260	88.7018	78.2313	64.5971	52.3562	42.3967	34.3626
Storage System	98.0340	98.0340	98.0340	98.0340	98.0340	98.0340	98.0340

Table 5.3: Subsystem reliability of PV system for 20 years of operations (in %) (using eq 2.20)

Power (in kW)	100	200	500	1000	1500	2000	2500
PV modules	66.5819	44.3315	13.3187	1.7428	0.2321	0.0304	0.0040
converter	27.1702	7.3822	0.1481	0.0008	0.0000	0.0000	0.0000
Inverter	8.3576	0.6985	0.0004	0.0000	0.0000	0.0000	0.0000
BOS	21.1485	9.0918	0.7372	0.0160	0.0002	0.0000	0.0000
Storage System	67.2253	67.2253	67.2253	67.2253	67.2253	67.2253	67.2253

is calculated for two different duration of operation: one year and 20 years and given in Tables 5.2 and 5.3 respectively. It is observed that with the increase in the PV power output, the reliability of the sub-assemblies and subsystems are decreased. It is observed that after one year of operation for a 200kW system, the PV module has 96.014% reliability measure that means probability of operating adequately, whereas the inverter subsystem has 78.024% reliability percentage. For 2MW system, the PV module has 66.69% probability of operating without failures, whereas the inverter has only probability of 9.46% as tabulated in Table 5.2. On the other hand, for 20 years of operation there is noticeable quick decline. For an instance, for 200kW system, the PV module has 44.33% reliability percentage, whereas the inverter has only 0.6985% reliability percentage. For 2MW system, the PV module has only 0.0304% probability of operating correctly, whereas inverter is having 0% of probability of operating without failure means it is not reliable as shown in Table 5.3.

When any one of the subsystems or sub-assemblies of the PV system fails then the reliability will be zero percent, the 0% reliability does not mean entire PV system failure. The entire system reliability for one year of operation is illustrated in Fig. 5.29 and the reliability for 20

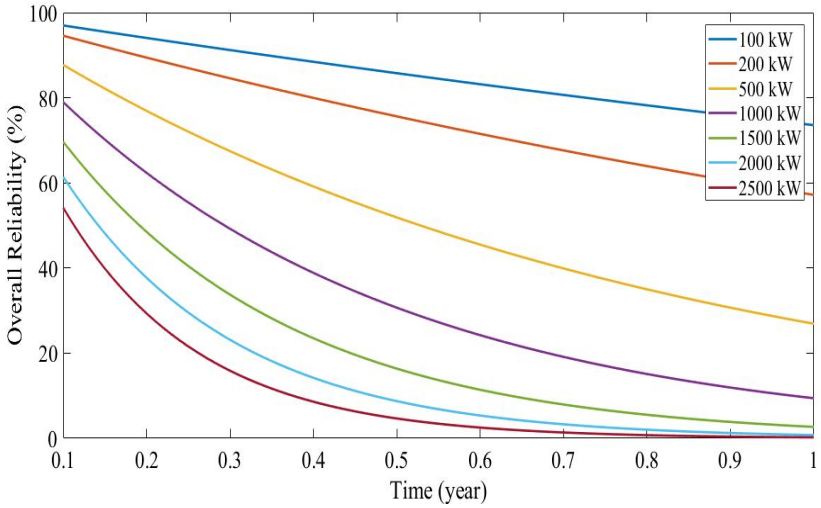

Figure 5.29: Percentage reliability of PV systems for one year of operation.

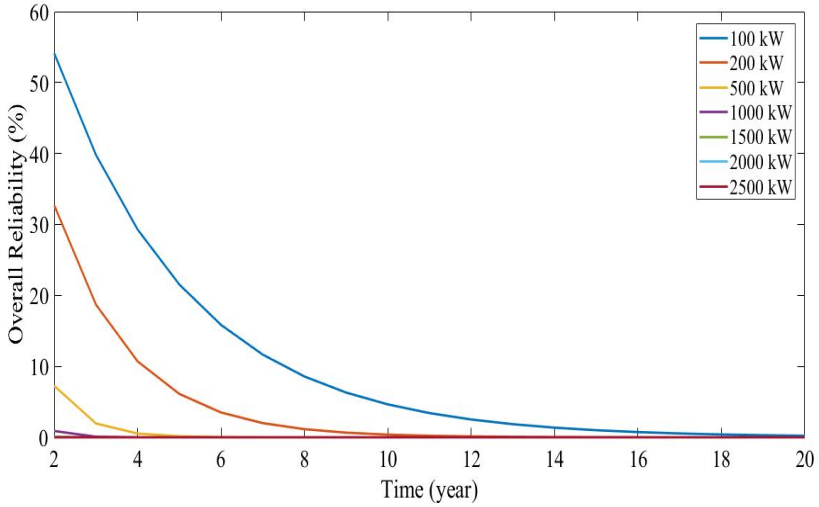

Figure 5.30: Percentage reliability of PV systems for 20 years of operation.

years of operation is illustrated in Fig. 5.30.

For estimating each sub system availability of PV system, the failure rates in the Table 2.3 and repair rates in the Table 2.4 are substituted into the eq 2.13 and the obtained values are listed in Table 5.4. From the Table 5.4, it is clear that the storage system is having the higher availability whereas the inverter system is having the lower availability when compared to the remaining five subsystems. The impact of availability of each subsystem on the entire system availability can be understood with the help of the availability importance measure. The availability importance measures for all the subsystems can be calculated by using eqs 2.15, 2.16, and 2.17 and then listed in Tables 5.5, 5.6, and 5.7.

Table 5.4: Subsystem availability (in %)

Power (in kW)	100	200	500	1000	1500	2000	2500
PV modules	99.8278	99.6562	99.1522	98.3115	97.4920	96.6791	95.8865
converter	99.9790	99.9580	99.8951	99.8114	99.7069	99.6026	99.4985
Inverter	98.1308	96.3303	91.3043	85.3659	78.9474	73.4266	68.6275
BOS	99.8690	99.7930	99.5678	99.2212	98.8494	98.4785	98.1123
System Storage	99.9603	99.9603	99.9603	99.9603	99.9603	99.9603	99.9603

Table 5.5: Availability importance measures

Power (in kW)	100	200	500	1000	1500	2000	2500
PV module	0.979428	0.960524	0.907783	0.845077	0.777793	0.719934	0.669677
Converter	0.977946	0.957623	0.901032	0.832378	0.760516	0.698803	0.645366
Inverter	0.996365	0.993687	0.985810	0.973232	0.960496	0.947921	0.935675
BOS	0.979024	0.959206	0.903994	0.837328	0.767113	0.706779	0.654484
System Storage	0.978130	0.957602	0.900445	0.831138	0.758588	0.696302	0.642385

From the Table 5.5, it can be observed that the components which are affecting the availability of solar PV system are PV module and inverter. Hence, it is clear that the overall availability of the system can be increased by improving the availability of the PV module and inverter of PV systems. From Tables 5.6 and 5.7, it is clear that the availability of each subsystem or component affects the overall availability of the system. This is possible to know using failure rate based and repair rate based availability importance measure method. From the results shown in Figs 5.31, 5.32, and 5.33, it is clear that inverter and PV module are the weakest components of the PV system. Therefore, these need to be given special attention for enhancing the overall availability of the PV system. Among the failure rate based and repair rate based availability measures techniques, the failure rate based availability measure method is more effective. Hence, it is given more focus to calculate the overall availability of PV system using failure rates of inverter and PV module.

To get the improved availability of the PV system, few solutions can be suggested as follows: preventive and predictive maintenance of the weakest components, reactive maintenance which involve the periodic inspection of the system components, and addition of redundant

Table 5.6: Importance measures based on failure rates

power (in kW)	100	200	500	1000	1500	2000	2500
PV Module	0.082790	0.080914	0.075699	0.069280	0.0627057	0.0570772	0.0522258
Converter	0.003151	0.003084	0.002898	0.002673	0.0024369	0.0022345	0.0020593
Inverter	0.147265	0.141529	0.126138	0.108856	0.0918840	0.0784418	0.0676378
BOS	0.016492	0.016525	0.015847	0.014806	0.0134831	0.0123412	0.0113475
System Storage	0.019567	0.019156	0.018013	0.016626	0.0151748	0.0139288	0.0128503

Table 5.7: Importance measures based on repair rates

power (in kW)	100	200	500	1000	1500	2000	2500
PV module	0.0001428	0.0002792	0.0006472	0.0011899	0.0016131	0.0019606	0.0022405
Converter	0.0000007	0.0000013	0.0000030	0.0000051	0.0000072	0.0000089	0.0000104
Inverter	0.0028050	0.0053916	0.0120131	0.0186611	0.0245024	0.0283885	0.0309201
BOS	0.0000216	0.0000343	0.0000688	0.0001162	0.0001569	0.0001907	0.0002183
System Storage	0.0000078	0.0000076	0.0000072	0.0000066	0.0000060	0.0000055	0.0000051

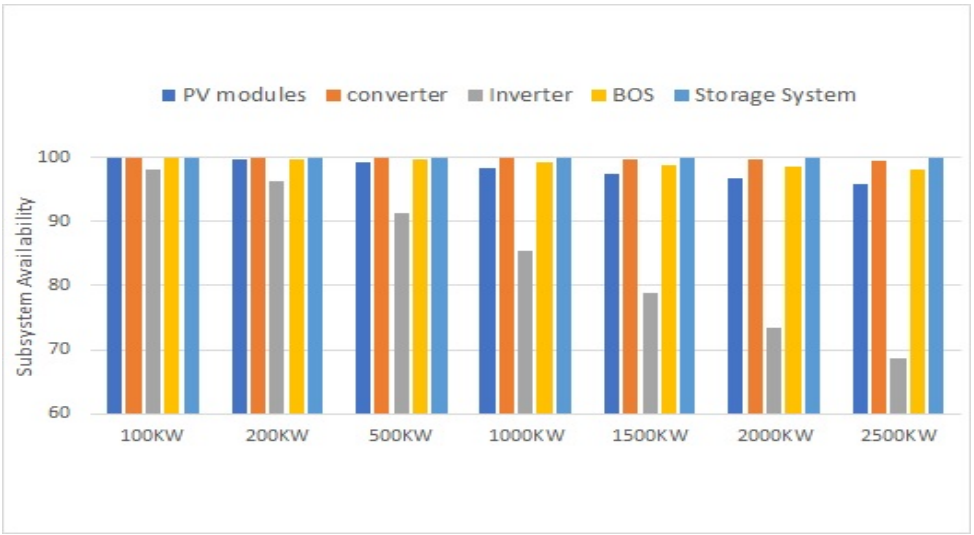

Figure 5.31: Sub-systems availability for the studied systems.

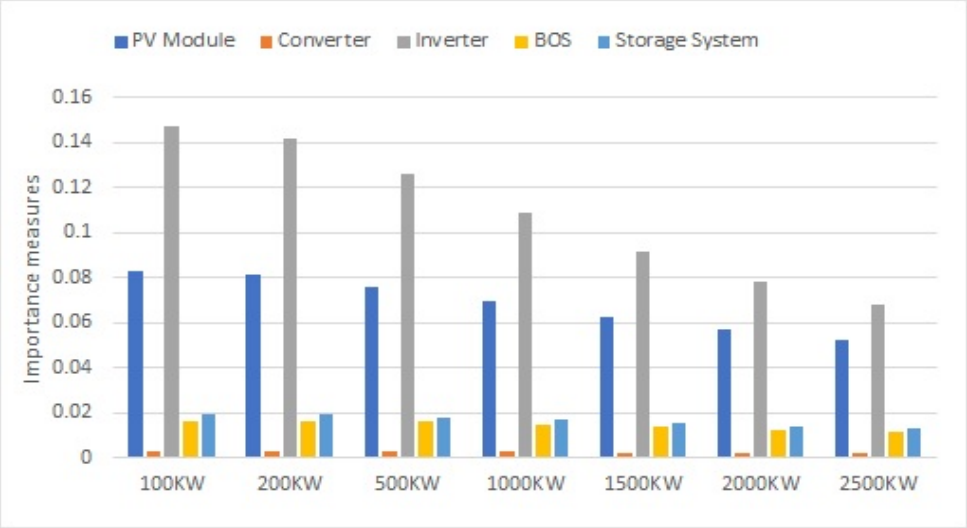

Figure 5.32: Importance measures for PV module, converter and inverter.

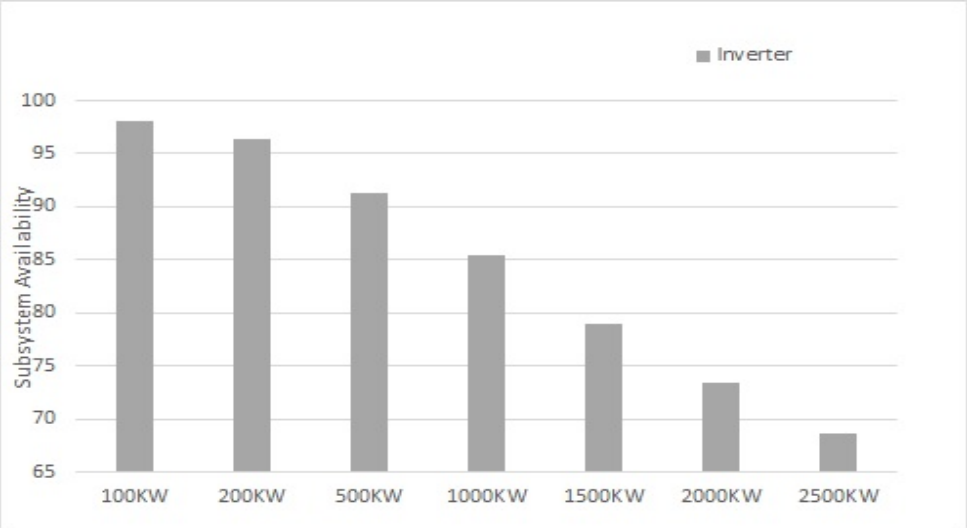

Figure 5.33: Sub-system availability for inverter.

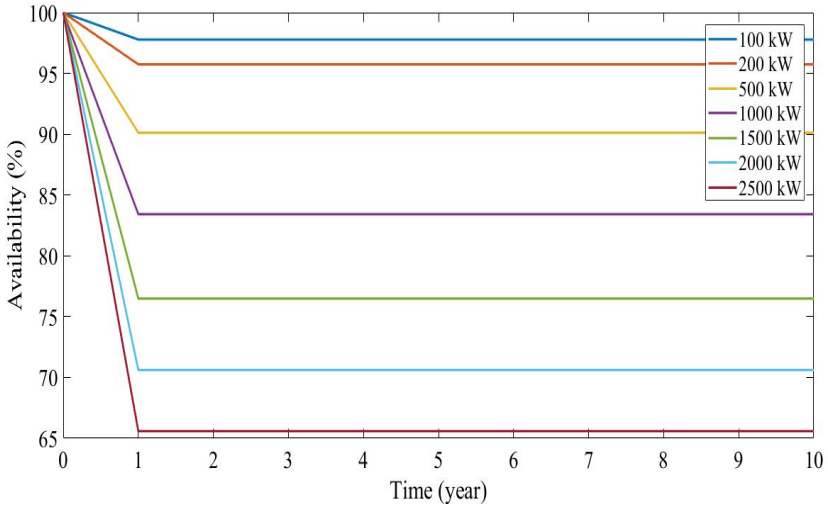

Figure 5.34: Overall system availability before inverter redundancy

systems.

By using redundancy approach for the weakest component of the PV system which is inverter, the availability of the entire system can be increased. Redundancy is nothing but adding new parallel paths. Redundant elements are energized continuously in a hot standby redundant system and made to perform the circuit function, whereas redundant elements perform if and only if the primary circuit elements fail in the cold standby redundancy. For a hot standby system, the failure rates and repair rates are given by the eqs 2.11 and 2.12 because redundancy means adding new parallel paths. With the help of eq 2.18, and Tables 2.3 and 2.4, the overall system availability is presented without redundancy and with redundancy of the inverter is presented in Figs 5.34 and 5.35. It can be observed that the entire system availability increases when inverter redundancy is considered as shown in the Figs 5.34 and 5.35.

In this chapter, only permanent faults that occur due to manufacturing defects which can be repaired manually if they occur are considered. Because of this, after one year the availability will not be affected by these faults that is it remains constant. From figs 5.34 and 5.35, it can be observed that the availability is constant after one year. Whereas there are other faults like intermittent which are not considered. If these faults also considered then the availability of the system may decrease continuously.

The results obtained from availability importance measures are tabulated in Table 5.5 which shows that the availability importance measure of inverter is highest for PV system. The most weakest component of PV system is the inverter having least reliability. The ranking

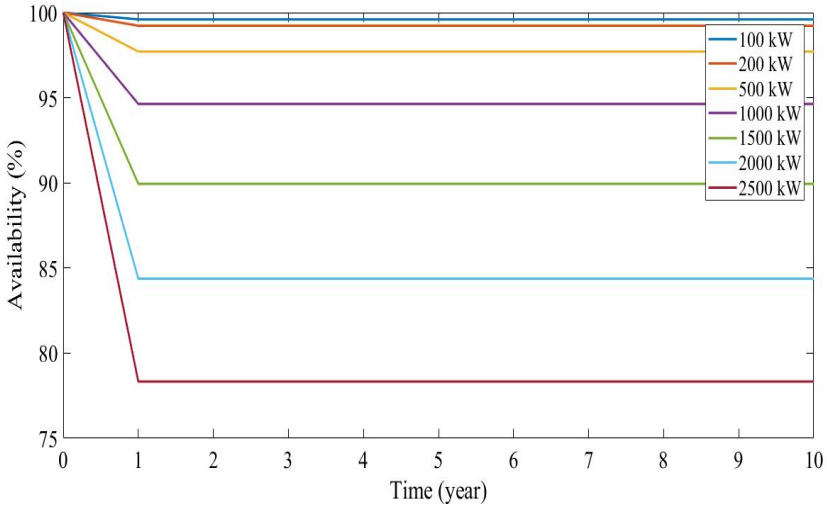

Figure 5.35: Overall system availability after inverter redundancy

Table 5.8: Ranking of components affecting the availability of PV system

Ranking	Subsystems of PV system
1	Inverters
2	PV modules
3	BOS
4	Converters
5	System Storage

of the subsystems based on their effect on the system availability are presented in Table 5.8.

The reliability values of the PV system found using proposed method and existing methods after one and twenty years of operation are shown in Tables 5.9 and 5.10 respectively.

The RACM of large PV systems is presented in this chapter. For the collected failure rate and repair rate data of various sub-assemblies, median based statistical method is used to improve the results of analysis. Elaborate analysis of the seven practical grid connected systems starting from sub-assemblies to subsystems then to the entire system by using the improved reliability block diagram has been carried out. Availability importance measures are calculated which have been used to find out the subsystem that have the greatest effect on the entire system availability. It has been found that entire system availability is mostly affected by the inverter subsystem. By using the availability importance measures, critical subsystems have been ranked based on their impact on the overall system availability. Regardless of the costs, the most

Table 5.9: Comparison of the reliability values of PV system found from proposed method and existing methods after one year of operation.

PV Systems (kW)	[42]	[8]	[6]	Proposed method
100	78.9735	78.3716	71.7895	71.6708
200	66.5429	65.2364	54.2866	52.3450
500	36.9867	36.3520	22.9058	22.0675
1000	16.0560	16.0188	7.0235	7.0083
1500	6.5542	6.3991	1.9056	1.8197
2000	2.2507	2.001	0.4663	0.41
2500	1.002	0.96	0.089	0.077

Table 5.10: Comparison of the reliability values of PV system found from proposed method and existing methods after twenty years of operation.

PV Systems (kW)	[42]	[8]	[6]	Proposed method
100	1.5192	0.6820	0.2800	0.1995
200	0.05	0.01	0.0008	0.0004
500	0	0	0	0
1000	0	0	0	0
1500	0	0	0	0
2000	0	0	0	0
2500	0	0	0	0

effective method to improve the system availability is to use redundancy method.

5.4 Summary

The work has discussed the WFC-SVM and WFC-KNN techniques, which can detect the OC faults in a single IGBT and multiple IGBTs of inverters. For feature extraction, the WF is found more accurate and simpler with least computational burden. KNN-based algorithm gives more accurate fault diagnosis results using the WFC feature of three-phase currents of the inverter as compared with SVM-based algorithm. The fault detection and localization time with the proposed technique are found in least time than the other techniques available in the literature and the techniques proposed in the previous chapters. The proposed WFC-KNN technique in this chapter is fit for implementing a fault diagnosis system to get reliable and faster fault detection schemes. The proposed methods (RBD with PCA, WE-SVM, EWP-SVM, WFC-KNN) are helpful in giving the complete condition monitoring of the system and the results obtained outperform the existing methods such as FTA and RBD. The condition monitoring of inverter which is the weakest component of PV system is presented in this thesis. The proposed condition monitoring algorithms are applicable in other sub-assemblies as well for improving the overall reliability and availability of the system which is future scope of this work.